Structural Eng. / Earthquake Eng. Vol. 3. No. 2, 225s-234s. October 1986
Japan Society of Civil Engineers (Proc. of JSCE No. 374/I-6)

NONLINEAR ANALYSIS OF THIN-WALLED STRUCTURES BY A COUPLED FINITE ELEMENT METHOD

By Toshitaka YAMAO and Tatsuro SAKIMOTO***

This paper presents a finite element method which enables to analyze a large displacement behavior of elasto-plastic thin-walled structures which fail by overall, local or interactive instability. An incremental equilibrium equation for a thin-walled beam-column is derived in a stiffness matrix form by using a moving element coordinate system and an incremental variational principle. So called multipoint constraints technique is used to connect plate elements with a beam element at the coupling nodal point in the cross section. Numerical results of the present method are compared with the exact solutions and experimental results. Validity and efficiency of the present method are confirmed.

Keywords : finite element method, thin-walled structures, elasto-plastic, large displacement analysis

1. INTRODUCTION

In the Japanese Specification for Highway Bridges[1], a relatively large width-to-thickness ratio of the component plates is allowed to use, when the working stress is smaller than the specified allowable stress. But, this does not mean that interaction behavior of local and overall buckling of thin-walled structures is well clarified. The interaction behavior of thin-walled structures is extremely complex. In paticular, it is not easy to find a theoretical solution for such a interaction problem including the effects of structural imperfections such as residual stresses and initial crookedness of the member. To the authors' knowledge, a practical method of analysis for these problems is not established yet.

Although many studies have been reported in reference to the local buckling behavior and the post-local-buckling strength of plates[2)~7)], most of those are analyses for a single plate element. Few have been studied on the maximum load carrying capacity of a structural member including the effects of interactive deformations between component plates of the cross section. The ultimate strength analyses for elasto-plastic thin-walled beam-columns with open cross section are also carried out as a beam element[8)~10)], but by these methods it is difficult to consider the effects of the local buckling of the plates in the analysis. Of course, it may be possible to carry out an elasto-plastic large displacement analysis by discretizing a whole structure into a large number of plate finite elements, but at present, it is obvious to encounter the difficulty resulting from a long computation time and extremely large memory capacity required for a digital computer.

The object of the paper is to present a formulation based on the finite element technique which enables us

* Member of JSCE, Ms. Eng., Research Associate, Department of Civil Engineering, Kumamoto University (Kurokami 2-chome, Kumamoto, 860)
** Member of JSCE, Dr. Eng., Professor, Department of Civil Engineering, Kumamoto University

to connect plate elements with a beam element. In the present analysis, the part where the local buckling is likely to occure is divided into plate elements, and the other parts are divided into beam elements. The part of plate elements is coupled with the part of beam elements at a cross section by a single nodal point. In this case, the total number of the freedoms of the plate elements lined up at the cross section is reduced to the same number as that of a beam element to be connected by introducing constraints[11] which satisfy the compatibility conditions. The technique is called coupling analysis in this paper. By this technique, the total number of freedoms can be reduced remarkably and the analysis for the interaction behavior of local and overall buckling of thin-walled structures become capable without much computational effort.

The beam element used in this method is the same one as given in Ref. 10) and has seven degrees of freedom. Constant in-plane strains and constant curvatures for plate bending are assumed in the plate element, but it is different from the ordinary planar triangluar element (5 degrees of freedom for one node) in the following point. That is, the in-plane flexural stiffness of the component plates is taken into account using a technique based on the micropolar theory[12] adopted by Suzuki et al.[6),7)]. Without this consideration for the in-plane flexural component of the plate, the stiffness matrix obtained may show singularity for spatial plate structures. By this consideration the number of freedom of the nodal point becomes six.

Since a large portion of the displacement in the postbuckling behavior of the plate element is caused by a rigid body displacement, the nodal forces are calculated by effective displacements which are determined by subtracting the rigid body displacement from the total one. To derive the incremental equilibrium equation, a moving element coordinate system and an incremental variational principle are used. Validity and efficiency of the present method are studied and shown in several numerical examples by changing the coupling location and number of discretized finite elements.

2. DERIVATION OF EQUILIBRIUM EQUATIONS

(1) Coordinate systems and assumptions

The basic assumptions used in the analysis are : a) the elasto-plastic behavior of the isotropic material can be modeled by the bi-linear stress-strain relationship between an equivalent stress and an equivalent strain, b) The von Mises yield criterion is acceptable and the stress-strain relationship of Prandtl-Reuss is valid in the inelastic range, c) The plane section perpendicular to the middle plane of the plate element remains plane after bending, d) The residual stress is constant within a plate element in its plane, but varies linearly through the thickness, e) The beam element has a thin-walled open cross section, and a plane section remains plane under the influence of flexural moment and a warping function used in the elastic theory of torsion is valid even after the initiation of yielding, f) The distribution of shear strain caused by Saint Venant torsion is linear through the thickness of section plate even for a partially yielded cross section, g) Local buckling of a beam element will not occur and distorsion of the cross section shape may be negligible in a beam element.

The local cartesian coordinate (x, y, z) for the plate element is set up as shown in Fig. 1 (a). The origin is chosen to be located at node number 1 and the z axis, which is then perpendicular to the middle plane of the plate 1, 2, 3, is taken upward positive. The x axis is taken along the side 12, and the y axis is taken perpendicular to the xz plane. The positive directions of the increments of nodal displacements and forces for the plate element in the local coordinate system are shown in Fig. 1 (a). The local cartesian coordinate is also set up for the beam element and fixed to the beam element. Positive directions of the vectors are shown in Fig. 1 (b).

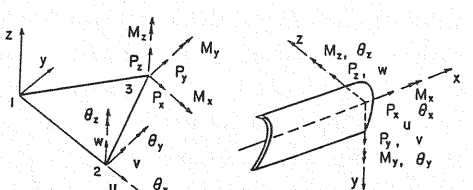

a) Plate Element b) Beam Element

Fig. 1 Element coordinate and increments of nodal forces and nodal displacements.

In the following derivation, the total quantities of displacements, forces, strains and stresses are denoted

by the letters with bars and the incremental quantities of those are denoted by the letters without bars.

(2) Tangent stiffness matrix for a plate element

The state of displacement of the middle plane of the plate element is defind by three displacement increments u, v and w in directions of the three axes x, y and z. Then the incremental strain vector ε_m, the incremental curvature vector ε_b, the incremental rotation vector ε_θ and incremental in-plane rotation vector ε_ϕ at the middle plane of the plate can be expressed by the incremental nodal displacement vector $\boldsymbol{u}_m$, $\boldsymbol{u}_b$ as follows:

$$\varepsilon_m=\begin{Bmatrix}\partial u/\partial x\\ \partial v/\partial y\\ \partial u/\partial y-\partial v/\partial x\\ 0\end{Bmatrix}=\boldsymbol{B}_m\cdot\boldsymbol{u}_m \quad\cdots\cdots(1)$$

$$\varepsilon_\phi=\begin{Bmatrix}0\\ 0\\ 0\\ 2\theta_z^*-(\partial v/\partial x-\partial u/\partial y)\end{Bmatrix}=\boldsymbol{B}_\phi\cdot\boldsymbol{u}_m \quad\cdots\cdots(2)$$

$$\varepsilon_b=\begin{Bmatrix}\partial^2 w/\partial x^2\\ \partial w^2/\partial y^2\\ 2\partial w^2/\partial x\partial y\\ 0\end{Bmatrix}=\boldsymbol{B}_b\cdot\boldsymbol{u}_b \quad\cdots\cdots(3)$$

$$\varepsilon_\theta=\begin{Bmatrix}\partial w/\partial x\\ \partial w/\partial y\end{Bmatrix}=\boldsymbol{B}_\theta\cdot\boldsymbol{u}_b \quad\cdots\cdots(4)$$

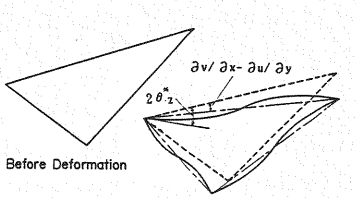

Fig. 2 The in-plane rotation.

where

$$\left.\begin{aligned}&\boldsymbol{u}_m=\langle\boldsymbol{u}_{m1}\ \ \boldsymbol{u}_{m2}\ \ \boldsymbol{u}_{m3}\rangle^T,\ \ \boldsymbol{u}_{mk}=\langle u\ \ v\ \ \theta_z\rangle_k^T\\ &\boldsymbol{u}_b=\langle\boldsymbol{u}_{b1}\ \ \boldsymbol{u}_{b2}\ \ \boldsymbol{u}_{b3}\rangle^T,\ \ \boldsymbol{u}_{bk}=\langle w\ \ \theta_x\ \ \theta_y\rangle_k^T\quad k=1\sim3\end{aligned}\right\}\quad\cdots\cdots(5)$$

in which the superscript T stands for transpose of the matrix, and the symbols $\{\ \}$ and $\langle\ \rangle$ denote the column vector and the row vector, respectively. The incremental in-plane rotation vector ε_ϕ is described herein as the difference between the micro rotation θ_z^* and the macro rotation as shown in Fig. 2. The displacement functions for in-plane displacements u, v and in-plane rotation θ_z are given by linear polynomials of x, y, and for out-of-plane displacement w by cubic polynomials of the area coordinates. The incremental strain vector ε of an arbitrary point in the plate element can be expressed by using Eqs. (1)~(4) as follows:

$$\varepsilon=\boldsymbol{B}_m\cdot\boldsymbol{u}_m+\boldsymbol{B}_\phi\cdot\boldsymbol{u}_m+1/2\cdot\boldsymbol{C}_\theta\cdot\boldsymbol{B}_\theta\cdot\boldsymbol{u}_b-z\boldsymbol{B}_b\cdot\boldsymbol{u}_b \quad\cdots\cdots(6)$$

where

$$\varepsilon=\langle\varepsilon_x\ \ \varepsilon_y\ \ \gamma_{xy}\ \ \gamma_\phi\rangle^T,\ \ \gamma_\phi=2\theta_z^*-(\partial v/\partial x-\partial u/\partial y),\ \ \boldsymbol{C}_\theta=\begin{bmatrix}\partial w/\partial x & 0\\ 0 & \partial w/\partial y\\ \partial w/\partial y & \partial w/\partial x\\ 0 & 0\end{bmatrix}\quad\cdots\cdots(7)$$

The incremental stress $\sigma=\langle\sigma_x\ \ \sigma_y\ \ \tau_{xy}\ \ \tau_\phi\rangle^T$ is related to the incremental strain vector by the stress-strain matrix $\boldsymbol{D}$ as

$$\sigma=\boldsymbol{D}\cdot\varepsilon \quad\cdots\cdots(8)$$

The matrix $\boldsymbol{D}$ can be expressed as the sum of the matrix for the elastic range $\boldsymbol{D}_e$ and the matrix for the inelastic range $\boldsymbol{D}_{ep}$. The matrix $\boldsymbol{D}_e$ can be written by Hooke's law as

$$\boldsymbol{D}_e=\frac{E}{1-\nu^2}\begin{bmatrix}1 & \nu & 0 & 0\\ \nu & 1 & 0 & 0\\ 0 & 0 & (1-\nu)/2 & 0\\ 0 & 0 & 0 & (1-\nu)/2\end{bmatrix}\quad\cdots\cdots(9)$$

in which E is Young's modulus and ν is Poisson's ratio. Assuming Prandtl-Reuss' equation and von Mises

yield criterion in the inelasic range, the matrix for the inelastic range $\boldsymbol{D}_{ep}$ can be expressed as follows :

$$\boldsymbol{D}_{ep}=\boldsymbol{D}_e-\frac{1}{S}\begin{bmatrix} S_x^2 & S_xS_y & S_xS_{xy} & 0 \\ S_yS_x & S_y^2 & S_yS_{xy} & 0 \\ S_{xy}S_x & S_{xy}S_y & S_{xy}^2 & 0 \\ 0 & 0 & 0 & S_{xy}^2 \end{bmatrix} \quad \cdots\cdots (10)$$

where

$$\left.\begin{aligned} &S_x=E(\sigma'_x+\nu\sigma'_y)/(1-\nu^2),\quad S_y=E(\nu\sigma'_x+\sigma'_y)/(1-\nu^2) \\ &S_{xy}=E\tau_{xy}/(1+\nu),\quad S=S_x\sigma'_x+S_y\sigma'_y+2S_{xy}\tau_{xy} \end{aligned}\right\} \quad \cdots\cdots (11)$$

in which σ'_x and σ'_y denote the deviation stress. In this analysis, the stress-strain relationship between the stress τ_ϕ and the strain γ_ϕ is assumed to be expressed in the same manner with the relationship the shear stress τ_{xy} and the shear strain γ_{xy} of the in-plane stress problems in both the elastic[6),12)] and inelastic[7)] ranges, and this relationship is considered to be independent of other stress-strain relationships.

When a plate element, starting from the initial state i subjected to the total external loads $\overline{\boldsymbol{p}}$, reaches to the subsequent state $i+1$ after producing increments of displacement due to the load increment $\boldsymbol{p}$, the incremental potential energy V during deformation is written as follows :

$$V=-\{(\overline{\boldsymbol{u}}+\boldsymbol{u})^T(\overline{\boldsymbol{p}}+\boldsymbol{p})-\overline{\boldsymbol{u}}^T\cdot\overline{\boldsymbol{p}}\}=-\boldsymbol{u}^T(\overline{\boldsymbol{p}}+\boldsymbol{p})-\overline{\boldsymbol{u}}^T\cdot\boldsymbol{p} \quad \cdots\cdots (12)$$

Assuming the linearity during an incremental step, the incremental strain energy U is given as

$$U=\int_V(\boldsymbol{\varepsilon}^T\overline{\boldsymbol{\sigma}}+1/2\,\boldsymbol{\varepsilon}^T\boldsymbol{\sigma})dV=\int_V\boldsymbol{\varepsilon}^T\overline{\boldsymbol{\sigma}}dV+1/2\int_V\boldsymbol{\varepsilon}^T\boldsymbol{D}\boldsymbol{\varepsilon}dV \quad \cdots\cdots (13)$$

After substitution of Eq. (6) into this equation, the increment of the potential energy $\pi=U+V$ can be written in terms of the increments of the nodal displacement $\boldsymbol{u}$. Since the stationary condition of π gives an incremental equilibrium condition, first partial derivatives of π with respect to $\boldsymbol{u}$ yield the following incremental equilibrium equation :

$$\boldsymbol{p}+(\overline{\boldsymbol{p}}-\overline{\boldsymbol{f}})=\begin{bmatrix} \boldsymbol{k}_{mm}+\boldsymbol{k}_{\phi\phi} & \boldsymbol{k}_{mb} \\ \boldsymbol{k}_{bm} & \boldsymbol{k}_{bb}+\boldsymbol{k}_g \end{bmatrix}\begin{Bmatrix} \boldsymbol{u}_m \\ \boldsymbol{u}_b \end{Bmatrix}=\boldsymbol{k}\boldsymbol{u} \quad \cdots\cdots (14)$$

where

$$\left.\begin{aligned} &\overline{\boldsymbol{f}}=\begin{Bmatrix} \overline{\boldsymbol{f}}_m+\overline{\boldsymbol{f}}_\phi \\ \overline{\boldsymbol{f}}_b \end{Bmatrix},\quad \overline{\boldsymbol{f}}_m=\int_V\boldsymbol{B}_m^T\overline{\boldsymbol{\sigma}}dV,\quad \overline{\boldsymbol{f}}_\phi=\int_V\boldsymbol{B}_\phi^T\overline{\boldsymbol{\sigma}}dV,\quad \overline{\boldsymbol{f}}_b=-\int_V z\boldsymbol{B}_b^T\overline{\boldsymbol{\sigma}}dV \\ &\boldsymbol{k}_{mm}=\int_V\boldsymbol{B}_m^T\boldsymbol{D}\boldsymbol{B}_m dV,\quad \boldsymbol{k}_{\phi\phi}=\int_V\boldsymbol{B}_\phi^T\boldsymbol{D}\boldsymbol{B}_\phi dV,\quad \boldsymbol{k}_{mb}=\boldsymbol{k}_{bm}^T=-\int_V z\boldsymbol{B}_m^T\boldsymbol{D}\boldsymbol{B}_b dV \\ &\boldsymbol{k}_{bb}=\int_V z^2\boldsymbol{B}_b^T\boldsymbol{D}\boldsymbol{B}_b dV,\quad \boldsymbol{k}_g=\int_V\boldsymbol{B}_\theta^T\overline{\boldsymbol{\sigma}}^*\boldsymbol{B}_\theta dV,\quad \overline{\boldsymbol{\sigma}}^*=\begin{bmatrix} \overline{\sigma}_x & \overline{\tau}_{xy} \\ \overline{\tau}_{xy} & \overline{\sigma}_y \end{bmatrix} \end{aligned}\right\} \quad \cdots\cdots (15)$$

The matrix $\boldsymbol{k}$ represents the tangent stiffness of the plate element. The matrix $\boldsymbol{k}_g$ is an initial stress matrix which represents geometrical nonlinearity caused by finite displacements. Since the matrices $\boldsymbol{k}_{mb}$ and $\boldsymbol{k}_{bm}$ are odd functions with respect to z, these matrices are zero in the elastic range but are not zero in the plastic range, because the stress-strain matrix $\boldsymbol{D}$ varies the value with z. The term $(\overline{\boldsymbol{p}}-\overline{\boldsymbol{f}})$ in Eq. (14) is considered as unbalanced forces caused by the linearization assumed in the formulation and by the yielding on the half way of an incremental load step.

(3) Tangent stiffness matrix for a beam element

Next, we derived an incremental equilibrium equation for a thin-walled beam element[10)]. Geometrical relations between the displacements and the rotation of the cross section are shown in Fig. 3. The axial strain increment ε of an arbitrary point $P(\eta,\ \zeta)$ on the cross section can be expressed by the displacement increments $(u,\ v,\ w)$ and the rotation increment ϕ of the arbitrary chosen reference point 0 as follows :

$$\varepsilon=u'-(\eta-\zeta\phi)v''-(\zeta+\eta\phi)w''+1/2\{(v')^2+(w')^2\}+1/2(\eta^2+\zeta^2)(\phi')^2+\omega\phi'' \quad \cdots\cdots (16)$$

in which a prime denotes a derivative with respect to x and ω denotes the normalized unit warping with respect to the point 0. The shear strain increment γ due to St. Venant torsion is given by

$$\gamma=2n\phi' \quad \cdots\cdots (17)$$

in which n is a coordinate originates at any point on the middle plane contour of the plate and is perpendicular of the coordinate s which is a tangent to the middle plane contour as shown in Fig. 3. The relationships between stress increments and strain increments can be given by the stress strain matrix D_b :

$$\begin{Bmatrix} \sigma \\ \tau \end{Bmatrix} = \boldsymbol{D}_b \begin{Bmatrix} \varepsilon \\ \gamma \end{Bmatrix} \quad \cdots\cdots (18)$$

The relationship between the increment of the resultant forces $\boldsymbol{r}$ and the corresponding deformation increment $\boldsymbol{d}$ is expressed by

$$\boldsymbol{r}=\boldsymbol{s}\cdot\boldsymbol{d} \quad \cdots\cdots (19)$$

where

$$\boldsymbol{r}=\langle P_x - M_z \;\; M_y \;\; M_w \;\; M_x\rangle^T, \quad \boldsymbol{d}=\langle u' - v'' \;\; -w'' \;\; \phi'' \;\; \phi'\rangle^T \quad \cdots\cdots (20)$$

in which the matrix $\boldsymbol{s}$ represents the tangent stiffness of a partially yielded member of unit length. The displacement functions employed herein are polynomials, which are usually used in an elastic finite element procedure. Namely u and v, w, ϕ are expressed by linear and cubic polynominals of x, respectively. The increment of the potential energy π can be written in terms of the increments of the nodal displacement $\boldsymbol{u}$. Since the stationary condition of π gives an incremental equilibrium condition, first partial derivatives of π with respect to $\boldsymbol{u}$ yeild the following incremental equilibrium equation :

$$\boldsymbol{p}+(\bar{\boldsymbol{p}}-\bar{\boldsymbol{f}})=(\boldsymbol{k}_{ep}+\boldsymbol{k}_g)\cdot\boldsymbol{u}=\boldsymbol{k}\cdot\boldsymbol{u} \quad \cdots\cdots (21)$$

The matrix $\boldsymbol{k}_{ep}$ represents the stiffness of an elasto-plastic member. The matrix $\boldsymbol{k}_g$ is an initial stress matrix which represents geometrical nonlinearity caused by finite displacements. Teh term $(\bar{\boldsymbol{p}}-\bar{\boldsymbol{f}})$ in Eq. (21) is considered as unbalanced forces. Details of the derivation and elements of matrices D_b, $\boldsymbol{s}$, $\boldsymbol{k}_{ep}$ and $\boldsymbol{k}_g$ are given in Ref. (10).

Transformation of Eqs. (14) and (21) to the global coordinate system by the ordinary transformation matrix $\boldsymbol{T}$ yields

$$\boldsymbol{K}\cdot\boldsymbol{U}=\boldsymbol{P}+(\bar{\boldsymbol{P}}-\bar{\boldsymbol{F}}) \quad \cdots\cdots (22)$$

where

$$\bar{\boldsymbol{F}}=\boldsymbol{T}\cdot\bar{\boldsymbol{f}}, \quad \boldsymbol{K}=\boldsymbol{T}^T\cdot\boldsymbol{k}\boldsymbol{T} \quad \cdots\cdots (23)$$

Equations obtained by assembling Eq. (22) for a whole structural system are the governing equilibrium equations to be solved.

(4) Coupling method by multipoint constraints[11]

The stiffness equation is generally given as follows :

$$\boldsymbol{P}=\boldsymbol{K}\cdot\boldsymbol{U} \quad \cdots\cdots (24)$$

in which $\boldsymbol{P}$ and $\boldsymbol{U}$ are the force vector and the displacement vector, respectively. The multipoint constraint equation is initially expressed in the following form.

$$\boldsymbol{R}\cdot\boldsymbol{U}=\boldsymbol{0} \quad \cdots\cdots (25)$$

in which $\boldsymbol{R}$ is the matrix of constraint coefficients. The displacement vector $\boldsymbol{U}$ is partitioned into two vectors $\boldsymbol{U}_n$ and $\boldsymbol{U}_m$. The vector $\boldsymbol{U}_m$ consists of displacements of dependent degrees of freedom and the vector $\boldsymbol{U}_n$ consists of displacements of independent degrees of freedom. Since the matrix $\boldsymbol{R}$ is similarly partitioned into $\boldsymbol{R}_n$ and $\boldsymbol{R}_m$, Eq. (25) can be written as

$$\boldsymbol{U}_m=-\boldsymbol{R}_m^{-1}\boldsymbol{R}_n\cdot\boldsymbol{U}_n=\boldsymbol{G}_m\cdot\boldsymbol{U}_n \quad \cdots\cdots (26)$$

in which $\boldsymbol{G}_m$ is called herein the coupling matrix. Prior to the imposition of constraints, Eq. (24) is partitioned in the following manner :

$$\begin{Bmatrix} \tilde{\boldsymbol{P}}_n \\ \boldsymbol{P}_m \end{Bmatrix} = \begin{bmatrix} \tilde{\boldsymbol{K}}_{nn} & \boldsymbol{K}_{nm} \\ \boldsymbol{K}_{nm}^T & \boldsymbol{K}_{mm} \end{bmatrix} \begin{Bmatrix} \boldsymbol{U}_n \\ \boldsymbol{U}_m \end{Bmatrix} \quad \cdots\cdots (27)$$

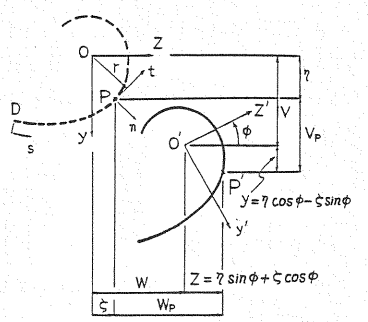

Fig. 3 Displacement of cross section.

A tilde over the symbol is used to denote matrices that are replaced in the reduction process. The addition of constraints to the displacement vector U_m requires to add the constraint force q_m to the equilibrium equations[27]. Since the constraint force q_m on U_m equals to additional force $-G_m^T q_m$ on U_m, we obtain the equilibrium and constraint equations together in partitioned form. That is,

$$\begin{Bmatrix} \tilde{P}_n \\ P_m \\ 0 \end{Bmatrix} = \begin{bmatrix} \tilde{K}_{nn} & K_{nm} & G_m^T \\ K_{nm}^T & K_{mm} & -I \\ G_m & -I & 0 \end{bmatrix} \begin{Bmatrix} U_n \\ U_m \\ q_m \end{Bmatrix} \quad \cdots\cdots (28)$$

where I denotes the unit matrix and q_m is the vector of constraint forces. Straightforward elimination of U_m and q_m yields

$$\{\tilde{P}_n + G_m \cdot P_m\} = [\tilde{K}_{nn} + K_{nm} \cdot G_m + G_m^T \cdot K_{nm}^T + G_m^T \cdot K_{mm} \cdot G_m] U_n \quad \cdots\cdots (29)$$

or

$$P_n = K_{nn} \cdot U_n \quad \cdots\cdots (30)$$

where

$$\left.\begin{aligned} K_{nn} &= \tilde{K}_{nn} + K_{nm} G_m + G_m^T K_{nm}^T + G_m^T K_{mm} G_m \\ P_n &= \tilde{P}_n + G_m^T P_m \end{aligned}\right\} \quad \cdots\cdots (31)$$

The initial partition of K and operations indicated by Eqs. (26) and (31) are performed by appropriate modules of the program. The derivation of the coupling matrix G_m for a H-section member shown in Fig. 4 is described as follows. The nodal point k of the beam element at which the plate element is connected has seven displacement components, u_k, v_k, w_k, θ_{xk}, θ_{yk}, θ_{zk}, θ'_{xk}. The nodal points ($1 \sim N$) of the plate element at this cross section are all dependent except for the independent nodal point k. Therefore, the displacement of the dependent nodal points of the plate element can be expressed by the displacement of the point k, according to the compatibility condition of displacement field of a thin-walled beam.

$$\left.\begin{aligned} u_i &= u_k - Y_i\theta_{zk} + Z_i\theta_{yk} - Y_i Z_i \theta'_{xk} \\ v_i &= v_k - Z_i\theta_{xk} \\ w_i &= w_k + Y_i\theta_{xk} \\ \theta_{xi} &= \theta_{xk} \\ \theta_{yi} &= \theta_{yk} - Y_i\theta'_{xk} \\ \theta_{zi} &= \theta_{zk} - Z_i\theta'_{xk} \qquad i = 1 \sim N \text{ (except } k\text{)} \end{aligned}\right\} \quad \cdots\cdots (32)$$

where Y_i and Z_i are the distance between each nodal point of the plate element and the coupled point k.

(5) Estimation of unbalanced forces

As for the estimation of unbalanced forces, the method developed by Kitada et al. in Ref. 4) are used in this analysis. Fig. 5 shows a nonlinear load-displacement relationship of a structure. On calculating the nodal force $\overline{F}_i$ of the state i after the i-th iteration from the equilibrium state M, it is necessary to calculate the incremental displacement U_M and the incremental strain from the equilibrium state M by using the total displacement $\overline{U}_i$ which is determined by subtracting the rigid body displacement from the total

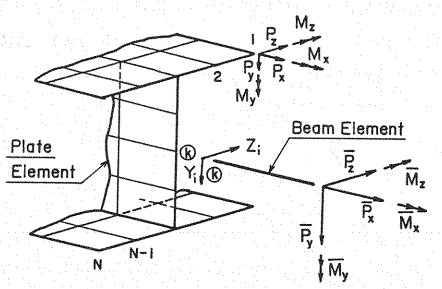

Fig. 4 Coupling nodal point.

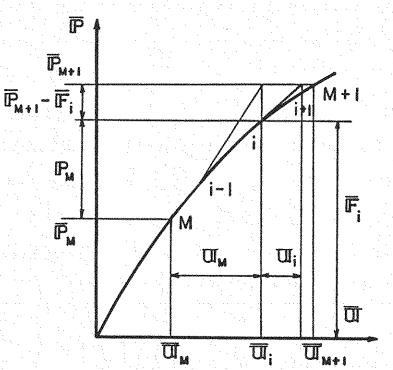

Fig. 5 Estimation of unbalanced forces.

displacement of the state i. Because if we use the incremental displacement calculated in each iteration in calculating the incremental strain, a trivial strain reversal which is nothing but a numerical phenomenon and has no relation to any actual strain reversal may occur. Therefore, the true incremental strains and stresses are determined by the incremental displacement $\boldsymbol{U}_M=\overline{\boldsymbol{U}}_i-\overline{\boldsymbol{U}}_M$.

The incremental nodal forces of each element for the state i are calculated by the incremental displacement $\boldsymbol{U}_M$, and added to the nodal forces of the state M. The sum is transformed to the global corrdinate and assembled for a whole element to obtain the nodal force $\overline{\boldsymbol{F}}_i$. The difference between the applied force $\overline{\boldsymbol{P}}_{M+1}$ and the nodal force $\overline{\boldsymbol{F}}_i$ is the unbalanced force which corresponds to the term $(\overline{\boldsymbol{P}}-\overline{\boldsymbol{F}})$ in Eq. (22).

(6) Computation procedure

In the computation, in order to analyze the development of plastic zone in the beam elements, the structure is divided into a number of member elements and cross sectional segments[10]. The rectangular plate element is considered as composed of four triangular elements and the stiffness of the rectangular element is determined as the average of the stiffness of the four triangular elements as shown in Fig. 6. The plate element is also divided into a number of layers to analyze the development of plastic zone, and the distribution of the stress and stress-strain matrix are assumed to be linear in each layer as shown in Fig. 7. The incremental equilibrium equation (22) operated by the multipoint constraints equation (31) is solved by using the Newton-Raphson procedure for the applied load increment. The procedure is repeated until the unbalanced force is eliminated and an equilibrium is obtained with the desired accuracy. The convergence in the computation is judged by the ratio of the displacement increments in the iterative step to the total displacements and the ratio of the unbalanced forces to the corresponding stress resultants. The computer program allows to use the load control method or the displacement control method in the Newton-Raphson procedure.

3. NUMERICAL EXAMPLES

Numerical examples for structures modeled by the beam elements are presented in Ref. 10) and the validity and efficiency of the method are confirmed. Therfore, the elasto-plastic analysis of the plate modeled by the plate elements is carried out as the first example. Then, thin-walled beam and column modeled by both plate elements and beam elements are studied by changing the coupling point location and the number of discretized finite elements.

(1) Elasto-Plastic square plate subjected to edge compression

A simply supported square plate with initial imperfections subjected to uniform compression in one direction is analyzed. The boundary condition at both unloaded edges is free with respect to the in-plane displacement. The initial central deflection w_0 is taken as 0.1 of the plate thickness t. The distribution of residual stresses is assumed to be rectangular and the magnitude of the stresses is assumed to be $\sigma_{rt}=$

Fig. 6 Rectangular plate element.

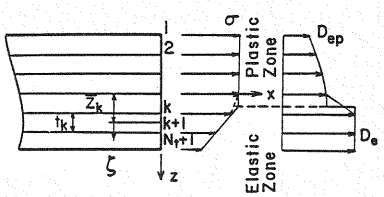

Fig. 7 Layer coordinate of plate element.

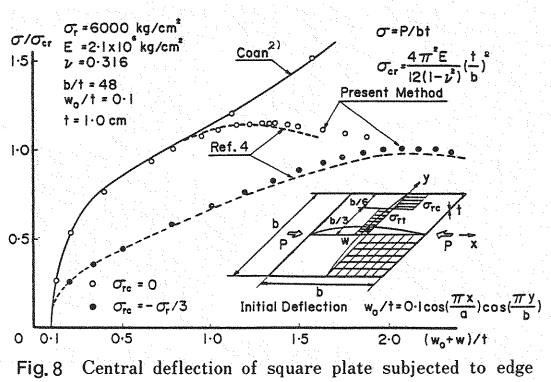

Fig. 8 Central deflection of square plate subjected to edge compression.

$-2\sigma_{rc}$ and constant along the direction of the applied load. The theoretical model is shown in the inset of Fig. 8 and a quarter part of the plate is analyzed considering double symmetry. The plate is divided into 6 elements along the width and length and each element further divided into 6 layers along the thickness. The uniform compression is applied in the computer program by giving uniform incremental displacements at the edges. Fig. 8 shows the load versus displacement diagrams. The vertical axis represents the mean axial stress σ divided by the elastic critical stress σ_{cr}. The horizontal axis shows the sum of the initial deflection w_0 and the additional lateral displacement w at the central point.

A solid curve in this figure is the exact solution as the elastic problem by Coan[2] and a broken lines is the results of the elasto-plastic analysis by Kitada et al.[4]. The result of the elastic analysis by the present method corresponds to the solution of Coan fairly well and the results of the elasto-plastic analysis by the present method correspond to the results of the Kitada et al. fairly well in both cases with and without the residual stress. The convergence with satisfactory accuracy is obtained after 5~6 repetitions in the iterative calculation.

(2) Large deflection of cantilever beam

Large deflection of an elastic cantilever beam with H-section subjected to the transverse load at the free edge is analyzed and the results are shown in Fig. 9. The part of the clamped side of the beam is modeled by the plate elements and the rest of the part is modeled by the beam elements. The flange plate of the former part is divided into 5 elements along the length and 6 elements along the width and the web plate is divided into 5 elements along the length and 4 elements along the width. The rest of the part is divided into 9 longitudinal beam elements. Each beam element is further divided into 192 cross sectional segments (8 divisions along the width or the height and 8 layers along the thickness for both flange and web plates). Since the aim of this example is to test the method for a large displacement behavior of the beam, imaginary material as described in the inset of Fig. 9 is assumed. The distance DL between the clamped end and the coupling point location is taken as 0.2 or 0.3 of the span length L[13]. Although the results of the present method vary slighty with the change of the coupling location DL, those show fairly good correspondence with the analytical solution by an elliptic integration. It is found from this example that even such a coarse discretization gives practically sufficient accuracy.

(3) Elasto-Plastic analysis of H-section column

Ultimate strength of a H-section column is analyzed and the results are shown in Fig. 10. The central part of the column is modeled by the plate elements and the rest of the part is modeled by the beam elements. The computation was carried out for the half of the column considering the symmetrical condition at the midheight. The manner and the number of the discretization are the same as the former example. The material properties and the initial crookedness are given as obtained by the experiment by Fujita et al.[14].

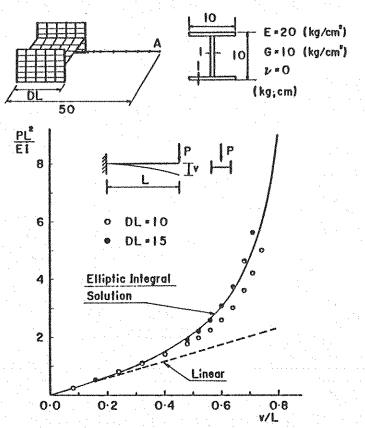

Fig. 9 Large deflection analysis of cantilever beam.

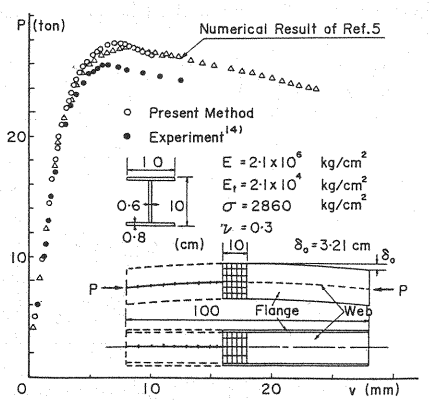

Fig. 10 Elasto-plastic analysis of H-section column.

The shape of the initial crookedness is assumed as the sine curve with the central value of 3.21 cm. The vertical axis P in Fig. 10 represents the compression load applied and the diflection v at the intersection point of the flange plate and the web plate at the midheight is plotted along the abscissa. The result of the present method corresponds to the finite element solution by Yoshida et al.[5] fairly well, but both results overestimate the maximum load of the column in comparison with the experimental result of Fujita et al.. The total number of the freedom of the equilibrium equation to be solved is 485 (DL=15) and 495 (DL=10) in the former example and 543 in this example. If we discretize whole of the half of the column into plate elements, the nodal points required to analyse increase by 9 times of those of the coupling model used herein. By this fact and the results shown in Fig. 10, the efficiency of the present method can be recognized. The axial compression at the end nodal point is given by controlling the incremental axial displacement in the computer program.

4. CONCLUSION

A finite element method with the multipoint constraints technique is developed for a useful analysis of a large displacement behavior of elasto-plastic thin-walled structures. The validity and efficiency of the present method are studied in the numerical examples and the following facts are confirmed. 1) Consideration of the in-plane flexural stiffness in the plate element makes it possible to analyze the structure composed of spatially assembled plates. 2) By using the method of subtracting the rigid body displacement, a large displacement behavior of the structure can be analyzed in surfficent accuracy. 3) The compatibility conditions at the coupling nodal point are satisfied sufficently and the efficiency of the multipoint constraints technique is shown. 4) The validity of the evaluation of the elasto-plastic tangent stiffness is confirmed. 5) Although the use of the plate element of constant in-plane strain makes the theoretical formulation easy, it should be noted that the results of the in-plane bending analysis of the plate is affected to some extent by the manner and number of the discretization both along the width and along the length of the plate.

The special advantage of the present method is that this method is able to analyze the behavior of the ultimate load carrying capacity of thin-walled structures considering the effects of local failure of the component plates without much increase in the number of the freedom of the equilibrium equation to be solved. Since the validity and applicability of the present method are well confirmed by the illustrative examples, it is now possible to investigate the complex interaction behavior of local and overall buckling of beam-columns etc. by using this coupling analysis.

The computations for numerical examples were conducted by digital computer FACOM M-382 of the Computer Center of Kyushu University. Part of this investigation was supported by the Funds of Aid for Scientific Researches from the Japanese Ministry of Education, Science and Cluture.

REFERENCES

1) Japan Road Association : Specification for Highway Bridges, Feb., 1980.
2) Coan, K.M. : Large Deflection Theory of Plates with Small Initial Curvature Loaded in Edge Compression, J. Appl. Mech., Vol. 18, Trans. ASME, Vol. 73, pp. 143~151, 1951.
3) Murray, D.W. and Wilson, E.L. : Finite-Element Postbuckling Analysis of Thin Elastic Plates, AIAAJ, Vol. 7, No. 10, Oct., 1969.
4) Komatsu, S., Kitada, T. and Miyazaki, S. : Elastic-Plastic Analysis of Compressed Plate with Residual Stress and Initial Deflection, Proc. of JSCE, No. 244, pp. 1~14, Dec., 1975 (in Japanese).
5) Yoshida, Y., Masuda, N. and Matusda, T. : A Discrete Element Approch to Elastic-Plastic Large Displacement Analysis of Thin Shell Structures, Proc. of JSCE, No. 288, pp. 41~55, Aug., 1979 (in Japanese).
6) Suzuki, T. and Kaneko, H. : A Large Deflection Analysis for Buckling and Postbudkling Behavior of Plate Elements of Structural Members by the Finite Element Method, Proc. of AIJ, No. 316, pp. 9~17, June, 1982 (in Japanese).
7) Suzuki, T. and Kaneko, H. : A Numerical Method for Elasto-Plastic Buckling Behavior of Coupled Plate Elements of Steel Structural Members, Proc. of AIJ, No. 323, pp. 23~31, Jan., 1983 (in Japanese).

8) Rajasekaran, S. and Murray. D. W. : Finite Element Solution of Inelastic Beam Equations, Proc. of ASCE, Vol. 99, No. ST6, pp. 1025～1041, June, 1973.
9) Epstein, M., Nixson, D. and Murray, D. W. : Large Displacement Inelastic Analysis of Beam-Columns, Proc. of ASCE, Vol. 104, No. ST5, pp. 841～853, May, 1978.
10) Sakimoto, T., Yamao, T., Kikuchi, R. and Sakata, T. : Nonlinear Analysis of Thin-Walled Frames and Members with Arbitrary Open Cross Sections, Proc. of JSCE, No. 362／(I-4), Oct., 1985.
11) Macneal, R. H. : The Nastran Theory of Manual, N. A. S. A., April, 1972.
12) Eringen, A. C. : Linear Theory of Micropolar Elasticity, J. Math. Mech., Vol. 15, pp. 909～923, No. 6, 1966.
13) Yamao, T., Hotta, M., Obata, K. and Sakimoto, T. : An Analysis of Thin-Walled Steel Structues by a Coupled Elements Technique, Proc. of 38th Annual Conference of JSCE, I-78, Sep., 1983 (in Japanese).
14) Fujita, Y., Yoshida, K. and Takazawa, M. : On the Strength of Structures with Imperfections (1st Report)-Compressive Strength of Columns with Initial Imperfections-, JSNAJ, No. 132, pp. 299～306, 1973 (in Japanese).

(Received October 14 1985)